Mason, Kelly E.; Oakley, Simon; Street, Lorna E.; Arroniz-Crespo, Maria; Jones, David L.; DeLuca, Thomas H.; Ostle, Nicholas J. 2019. **Boreal forest floor greenhouse gas emissions across a Pleurozium schreberi-dominated, wildfire-disturbed chronosequence**.

This is a post-peer-review, pre-copyedit version of an article published in *Ecosystems*, 22 (6). 1381-1392. The final authenticated version is available online at: https://doi.org/10.1007/s10021-019-00344-2.

Boreal forest floor greenhouse gas emissions across a *Pleurozium schreberi*-dominated, wildfire-disturbed chronosequence

Shortened title for page headings: Boreal forest floor GHG fluxes in later succession

Kelly E. Mason,[1*] Simon Oakley,[1] Lorna E. Street,[2] María Arróniz-Crespo,[3,4] David L. Jones,[4]
Thomas H. DeLuca,[5] and Nicholas J. Ostle[6]

[1]*Centre for Ecology & Hydrology, Lancaster Environment Centre, Library Avenue, Bailrigg, Lancaster LA1 4AP, UK*
[2]*School of GeoSciences, University of Edinburgh, Edinburgh, UK*
[3]*Departamento de Química y Tecnología de Alimentos, Universidad Politécnica de Madrid, Madrid, Spain*
[4]*School of Environment, Natural Resources and Geography, Bangor University, Bangor, UK*
[5]*WA Frank College of Forestry and Conservation, University of Montana, Missoula, USA*
[6]*Lancaster Environment Centre, Lancaster University, Lancaster LA1 4YQ, UK*

Abstract

The boreal forest is a globally critical biome for carbon cycling. Its forests are shaped by wildfire events that affect ecosystem properties and climate feedbacks including greenhouse gas (GHG) emissions. Improved understanding of boreal forest floor processes is needed to predict the impacts of anticipated increases in fire frequency, severity, and extent. In this study, we examined relationships between time since last wildfire (TSF), forest floor soil properties, and greenhouse gas emissions (CO_2, CH_4, N_2O) along a *Pleurozium schreberi*-dominated chronosequence in mid- to late succession located in northern Sweden. Over three growing seasons in 2012-2014, GHG flux measurements were made *in situ* and samples were collected for laboratory analyses. We predicted that *P. schreberi*-covered forest floor GHG fluxes would be related to distinct trends in the soil properties and microbial community along the wildfire chronosequence. Although we found no overall effect of TSF on GHG emissions, there was evidence that soil C:N, one of the few properties to show a trend with time, was inversely linked to ecosystem respiration. We also found that local microclimatic conditions and site-dependent properties were better predictors of GHG fluxes than TSF. This shows that site-dependent co-variables (i.e. forest floor climate and plant-soil properties) need to be considered as well as TSF to predict GHG emissions as wildfires become more frequent, extensive and severe.

Key words: boreal forest; wildfire disturbance; greenhouse gas emissions; carbon dynamics; forest floor; chronosequence

Introduction

Occupying 11% of the global land surface, boreal forests represent Earth's largest terrestrial biome and provide habitats for uniquely adapted biodiversity (Wardle and others 2003). These forests are estimated to hold 32% of global forest ecosystem carbon (C) stocks (Pan and others 2011) and play a major role in global greenhouse gas (GHG) dynamics (McNamara and others 2015). Wildfire is a major driver of change in the boreal region, turning the forest from a sink to a source of C through its release to the atmosphere, mainly in the form of CO_2 but also as methane (CH_4), carbon monoxide, and particulate C (Flannigan and others 2005). However, there is currently little information on how wildfire history influences forest floor GHG emissions.

Boreal forests are also particularly vulnerable to climate change with warming and reduced precipitation predicted to lengthen the fire season, increase fuel load, and reduce fuel moisture (Kovats and others 2014). These conditions have the potential to increase the frequency, intensity, severity, and extent of wildfires in the boreal region (de Groot and others 2013; Flannigan and others 2013), although fire suppression by human activity and land-use change may counteract this to some degree (Niklasson and Granstrom 2000; Girardin and others 2009). Understanding the mechanisms underpinning the recovery of these ecosystems is important for predicting how an overall increase in fire activity will contribute to global GHG emissions.

Boreal forests are characteristically nutrient poor, but fire releases nutrients, such as nitrogen (N), locked up in living biomass back into the system (Harden and others 2002; DeLuca and others 2002a; 2008). In the years following burning, this nutrient flush is essential for the growth of new biomass and recovery of C stocks. This fertile early successional stage, with plant communities of high litter quality and rapid turnover supporting belowground microbial biomass and decomposition processes (Wardle and Zackrisson 2005), transitions into a slower stage of recovery after several decades (Chapin and others 2002, Ward and others 2014).

In later succession, decreasing nutrient availability slows the growth of biomass and leads to changes in the forest floor plant communities, upon which belowground activity is highly dependent (Wardle 1997). In these stands, forest floor vegetation is dominated by slow-growing species with more recalcitrant litter. In particular, the feather mosses *Pleurozium schreberi* (Bird.) Mitt and *Hylocomium splendens* can take several decades to establish but then often cover up to 70-100% of the ground surface (Engelmark 1999; DeLuca and others 2002a; Zackrisson and others 2004; Street and others 2013). These mosses contain N-fixing cyanobacteria that contribute to the accumulation and cycling of an otherwise limiting nutrient in the system (DeLuca and others 2002b; Zackrisson and others 2009) and influence belowground microbial processes by altering conditions such as soil moisture and temperature (Oechel and Van Cleve 1986; Bonan and Shugart 1989; Williams and Flanagan 1996).

Despite substantial work done to understand forest floor ecosystem properties in a post-fire chronosequence of forested Swedish boreal islands that have not experienced fire for hundreds up to thousands of years (for example, Wardle 1997; Wardle and others 2003, 2012a, 2012b; Lagerström and others 2009; Clemmensen and others 2013, 2015; McNamara and others 2015), only a few studies have looked at trends in post-fire forest floor recovery in the wider boreal landscape of northern Europe (Zackrisson and others 1996; DeLuca and others 2002a, Zackrisson and others 2004), where the fire return interval is approximately 200-300 years (Carcaillet and others 2007). Although some evidence suggests that rapid early changes in forest floor ecosystem properties reach a “steady state” several decades after fire (Ward and others 2014), other evidence shows that more gradual changes continue over longer periods of time (Paré and others 1993; DeLuca and others 2002a; O’Neill and others 2003; Zackrisson and others 2004). To date, no studies have examined the relationship between *in situ* GHG fluxes and boreal forest floor properties across a wildfire chronosequence in mid- to late succession in northern Europe.

In this study, we wanted to determine the relationships between time since last wildfire (hereafter ‘time since fire’, TSF), soil properties, and forest floor GHG emissions of CO_2, CH_4, and N_2O in

Pleurozium schreberi-dominated boreal forest stands in mid-late succession. We achieved this using a wildfire-disturbed chronosequence located in northern Sweden consisting of six sites ranging from 47 to 367 years since last wildfire. These sites form part of a larger chronosequence used in previous works, which have shown increased feathermoss cover and associated N-fixation with increasing TSF, as well as reduced nitrification, ammonification, and N mineralization (DeLuca and others 2002a, Zackrisson and others 2004). We collected forest floor samples and measurements during the growing season over three years between 2012 and 2014. Our objectives were to explore whether *P. schreberi* had an effect on forest floor GHG emissions with increasing TSF and to examine whether changes in forest floor soil properties and local climatic factors account for variance in these GHG emissions. We hypothesized TSF would be an important predictor of *P. schreberi*-dominated forest floor GHG fluxes as a result of associated changes in soil properties. Specifically, we expected that with increasing TSF, CO_2 fluxes would increase with the buildup of the organic soil horizon, CH_4 influx would increase as in McNamara and others (2015), and that N_2O fluxes would increase in relation to increased *P. schreberi* cover and associated increases in N_2-fixation.

Methods

Field sites and microclimate measurements

The field sites for this project were located in the Northern Boreal zone of Sweden. They comprised a subset of six forest reserve stands of varying age since last wildfire (i.e. 47-367 years) selected from a chronosequence of sites that had previously been dated using tree ring scars (Zackrisson 1980) (Table 1; site ages are TSF as of 2014). The sites were selected at locations with a similar soil type (developed in granitic glacial till or sediment, with a 2-10 cm thick Oa/Oe horizon, 10-20 thick cm E horizon, and 30-40 cm thick Bs horizon, classified as either Typic or Entic Haplocryods; DeLuca and others 2002a) and vegetation composition (i.e. Scots pine (*Pinus sylvestris*), Norway spruce (*Picea abies*)), and a ground vegetation of dwarf shrubs (i.e. *Vaccinium* sp., *Empetrum* sp., and *Calluna* sp.) and feather mosses (i.e. *P. schreberi* and *H. splendens*)). Weather stations measuring air temperature, soil temperature at 1 cm and 5 cm depth, soil moisture, and surface leaf moisture (Decagon Devices, Inc, USA) were installed at all sites. Microclimate data was collected between June 2012 and July 2014.

Forest floor greenhouse gas fluxes

To measure forest floor greenhouse gas fluxes (i.e. excluding trees), five permanent PVC collars (30 cm diameter, 10 cm height) were installed along a 50-100 m transect at each site. Collar locations were selected at 10-20 m distance intervals, on a mat of *P. schreberi*. These were left for two days before the first sets of GHG flux measurements were made. Plots were sampled once in June 2012 and twice in each following sampling campaign (September 2012, June 2013, and July 2014). Gas fluxes were measured following the methods of Ward and others (2013). Briefly, forest floor ecosystem respiration (ER) and net ecosystem exchange (NEE) were measured over 2 minute intervals using a portable infrared gas analyser (PP Systems EGM4) connected to an opaque or clear chamber lid (35 cm height), respectively. For NEE, measurements were made of photosynthetically active radiation (PAR) at the height of forest floor vegetation using a PAR Quantum Sensor (Skye Instruments, UK). NEE is the combination of ER and gross primary productivity (GPP), such that a negative value for NEE indicates that GPP is greater than ER (i.e. CO_2 is being sequestered) while a positive value indicates that ER is greater (i.e. net CO_2 is being released). Forest floor CH_4 and N_2O fluxes were measured using a closed static chamber approach, whereby opaque chamber lids were sealed and headspace samples (10 mL) were taken using a gas syringe every ten minutes over half an hour and immediately injected into evacuated 3 mL Exetainer® vials (Labco Ltd, UK). Samples were analysed in the laboratory on a PerkinElmer Autosystem XL gas chromatograph (GC) with an FID for CH_4, an electron capture detector for N_2O and argon carrier gas. Sample peak areas were converted to part per million (ppm) concentrations using a standard curve based on three calibrated gas standard mixtures (BOC, UK). Results were corrected for instrumental drift as required. Gas concentration data from the GC were transformed from parts per million to flux of mg CH_4-C or mg N_2O-N m^{-2} hr^{-1}. Quality control procedures were implemented to identify missing data values or effects of atmospheric contamination of stored samples (all methods from Ward and others 2013).

Plant and soil sampling and analyses

Following the final round of GHG flux sampling in 2014, gas sampling plots were destructively harvested. All aboveground plant material within the gas chamber collars was collected, dried at 60ºC, and weighed for total dry weight biomass. One soil core (5 cm diameter, 10 cm depth) was taken from the centre of the collar to measure soil horizon depth, bulk density, and total soil C and N content. Estimates of cover by individual plant species were made where plants were often overlaid, creating >100% cover. In June 2012, six soil cores were collected along a transect for measurements of inorganic nitrogen (i.e. NO_3^-, NH_4^+). In September 2013, four additional cores were collected for analysis of more soil properties, including pH, total phosphorous (P), loss on ignition (as a measure of organic matter content), and microbial PLFA content (as described below) of the soil organic horizon at each site.

To determine microbial biomass and fungal/bacterial ratios, soil samples were extracted following a modified Bligh and Dyer (1959) method, as described by Crossman and others (2004). Briefly, lipids were extracted from freeze-dried, finely ground soil samples using Bligh and Dyer extractants and a citrate buffer, then separated into neutral, free fatty acids, and phospholipids on a silica solid phase extraction column. Mild alkaline methylation of the phospholipids produced fatty acid methyl esters for analysis. Once suspended in hexane, 1 µL PLFA samples were analysed on an Agilent Technologies (UK) 6890 GC equipped with a CP-Sil 5CB fused-silica capillary column (50 m x 0.32 mm i.d. x 0.25 µm) and flame ionization detector (FID). Sample PLFA peaks were identified based on known relative retention times, calculated as a proportion of the internal standard C19:0 methyl nonadeconoate, and converted to nmol PLFA g_{dw}^{-1}. Bacterial PLFAs were identified by terminal and mid-chain branched fatty acids (15:0i, 15:0a, 16:0i, 17:0i, 17:0a) or cyclopropyl saturated and monosaturated fatty acids (16:1ω7, 7,cy-17:0, 18:1ω7, 7,8cy-19:0), while fungal PLFAs were identified as 18:2ω6,9. The concentration of total PLFAs was calculated using all identified peaks (Whitaker and others 2014).

Statistical analysis

Statistical analyses were executed to determine the significance of a) relationships between TSF and site forest floor properties, and b) key ecosystem properties as predictors of forest floor GHG emissions. All statistical analyses were performed in R software (R Development Core Team 2014).

Soil and plant properties along the chronosequence

Linear regression analyses were carried out to determine trends in some forest floor properties with increasing TSF. These were carried out on soil collected both from within the gas sampling collars and along the transects, as well as on *P. schreberi* cover and total aboveground biomass from within the sampling rings. If required, data were transformed to meet model assumptions. To correct for multiple comparisons, a false discovery rate (FDR) correction was applied to *p*-values using the Benjamini-Hochberg critical value for FDR of 0.25.

Linear mixed effects modelling to predict GHG fluxes

Linear mixed effects (LME) models were developed to examine controls on forest floor GHG fluxes. Before looking at more complex models, we created simple LME models for individual sampling campaigns to determine trends in GHG fluxes with increasing TSF (nlme package, Pinheiro and others 2015). For this, GHG flux response was modelled with TSF as a fixed effect and plot as a random effect for repeated sampling. Again, data were transformed where necessary to meet model assumptions and the FDR correction was applied to *p*-values. Parameter estimates were obtained through a restricted maximum likelihood (REML) estimation of the models. *P*-values were obtained through likelihood ratio tests of each model compared to the same model minus TSF as a fixed effect, both created using a maximum likelihood (ML) estimation. R^2 values for each model were obtained using the MuMIn package (Bartoń 2016)

Following the simple mixed effects modelling procedure, it was determined that the GHG flux responses measured did not show any consistent trends with increasing TSF; therefore, two sets of models containing the other measured parameters were subsequently developed: one set containing TSF (continuous) as a fixed effect, and the other set using site (discrete).

The models were developed using the following approach. To begin, a correlation matrix was used to identify factors showing collinearity (>70% correlated) and one of each collinear pair was excluded from the initial model. To examine the effects of site-specific microclimates on forest floor greenhouse gas fluxes, weather station data was incorporated into the LME models. This, however, meant data was reduced to five sites as GUO had no weather station. After removing collinear weather station variables, we included the following data averaged over one hour prior to sampling: mean soil temperature at 5 cm depth, mean soil moisture, and mean surface leaf moisture. Although plant species cover was recorded, only final aboveground biomass and percent cover of *P. schreberi* were included in the models due to collars being placed selectively on *P. schreberi* mats rather than randomly, covering natural variation in plant cover. The final selection of factors included in the initial models are summarized in Table 2. Next, random effects were included in the models to account for repeated sampling at each plot and unequal variances between sites (Zuur and others 2009). Using ML estimations, fixed effects selection was performed using single term deletions and chi-squared likelihood ratio (LR) tests, where factors with non-significant effects ($p > 0.05$) were sequentially removed from the model. Again, likelihood ratio deletion tests (LRTs) determined the significance of retained factors by comparing the selected model with that same model but with the factor removed. If single terms were included in significant interactions, the interaction was also dropped before testing LRs (Zuur and others 2009; De Vries and others 2012). Finally, the models were fit using REML estimations to obtain parameter estimates.

Results

Soil properties and plant composition

We measured a range of soil metrics to determine whether differences in soil organic horizon properties underlying mats of *P. schreberi* differed across the chronosequence. Linear regression analyses showed C:N at these six sites to increase with TSF, both within the GHG rings ($R^2 = 0.153$, $p < 0.033$) and from the other samples taken along the transects ($R^2 = 0.233$, $p < 0.020$). Also from samples taken along the transects, total N ($R^2 = 0.181$, $p < 0.043$) and NH_4^+ ($R^2 = 0.190$, $p < 0.008$) decreased with increasing TSF; however, this was not seen in the samples taken from the GHG rings (Figure 1). No other properties showed significant changes with TSF (Figure S1).

Measurements of plant aboveground biomass and percent cover of *P. schreberi* were taken from within the gas sampling rings at each site. Total aboveground biomass did not change with TSF, while *P. schreberi* cover ranged from 70-100% in the youngest site and increased to 100% in the two oldest sites (Figure S2).

Greenhouse gas fluxes

The results of simple mixed effects models on the various GHG fluxes with age are presented in Figure 2. Mean rates of ER were in the range of 20 to 120 mg CO_2-C m^{-2} hr^{-1}. July 2014 showed higher overall fluxes and was the only sampling campaign to show a trend for ER (decreasing) with increasing TSF (-0.144*$year^{-1}$ ± 0.04 (SE), $R^2_{marginal} = 0.204$, $df = 4$, $p < 0.001$). Mean NEE fluxes ranged from about -42 to +33 mg CO_2-C m^{-2} hr^{-1}, where negative values equate to a net sink and positive values represent a net source of CO_2. In June 2013 alone, NEE showed a slight but weak increasing trend with TSF (0.098*$year^{-1}$ ± 0.048 (SE), $R^2_{marginal} = 0.084$, $df = 4$, $p < 0.049$). Mean methane flux rates were all negative, ranging from approximately -73 to -2 µg CH_4-C m^{-2} hr^{-1}, suggesting a net oxidation of CH_4. Regression analyses showed weak trends of small increases in CH_4 flux with stand TSF in June 2013 (0.063*$year^{-1}$ ± 0.031 (SE), $R^2_{marginal} = 0.097$, $p < 0.039$) and July 2014 (0. 108*$year^{-1}$ ± 0.050 (SE), $R^2_{marginal} = 0.127$, $p < 0.030$). N_2O fluxes ranged from -3 to +4 µg N_2O-N m^{-2} hr^{-1} and did not vary significantly across sites.

Because there was not a consistent linear effect of TSF on soil properties or GHG fluxes, we have focussed on presenting GHG flux models created using site (discrete) rather than TSF. However, results of the flux models created using TSF are presented in Tables S1-S2. No significant model was found for N_2O fluxes when TSF was used as a fixed effect.

The model results (using site) for the different gas fluxes are summarized in Tables 3 and 4. The site x soil temperature interaction was significant for NEE, with soil temperature correlated with increases in NEE (i.e. lower uptake of CO_2). Site was a significant factor for ER, CH_4, and N_2O fluxes. ER, NEE, and CH_4 flux also varied across different sampling campaigns. Related to recent condensation and precipitation, increases in mean leaf surface moisture around the time of sampling were negatively related to ER and CH_4 flux but positively related to N_2O flux; however, increased soil moisture was strongly associated with higher ER and also linked to lower N_2O. Soil properties were significant in only two of the GHG flux models (Table 3); ER was negatively related to C:N while NEE decreased (i.e. higher uptake of CO_2) with increased organic horizon depth.

Discussion

In this study, we set out to determine whether soil properties of *P. schreberi*-dominated boreal forest stands in mid- to late succession show patterns of change that could be used along with TSF and microclimatic data to predict forest floor GHG fluxes. We found that properties of the soil organic horizon, to which post-fire changes to soil C and nutrients are largely restricted (Holden and others 2013), varied amongst the six sites. There were some weak trends in soil properties with TSF; C:N showed a small increase with time since fire while NH_4^+ and total N content decreased. Due to equipment, logistical, and time limitations associated with closed-chamber gas sampling, we were forced to select six chronosequence sites, so it is likely that the number and age range of our sites were not great enough to capture many significant differences. In a prior study using this chronosequence, eight sites (including three from this study) were used and some differences in soil variables were indeed observed with TSF (DeLuca and others 2002a). Of the few observed changes in soil properties with increasing TSF, the increasing ratio of C to N was associated with lower ER fluxes in our study. This result indicates that higher natural soil N is associated with enhanced soil microbial activity, which has been seen with N addition studies in other low-N systems (Jonasson and others 1999; Allison and others 2008). However, there was no such relationship observed with total N, and some research suggests that total C:N is not a good indicator of humus decomposition, which can be more dependent on the quality of C rather than N availability (e.g. bound up in N-polyphenol complexes that inhibit production of complex-C degrading enzymes) (Prescott and others 2000; Hobbie and others 2002; DeLuca and Boisvenue 2012).

We found that forest floor GHG fluxes showed minor, intermittent trends across the wildfire chronosequence. There was some evidence of decreased ER and increased NEE on two separate sampling campaigns. The decrease in the influx of CH_4 with increasing TSF, as observed on two sampling campaigns, was small but statistically significant. This is contrary to the results of McNamara and others (2015), who found an increase in the CH_4 sink capacity of boreal soils with increasing TSF in the aforementioned chronosequence of island sites in northern Sweden. One reason for this could be in part due to the higher amount of *P. schreberi* cover in older stands, as some mosses are known to emit small amounts of CH_4 (Lenhart and others 2015).

The site x soil temperature interaction was significant in the LME model of NEE, suggesting that the effect of a rise in temperature varied from site to site. One explanation for this could be that the temperature sensitivities (Q_{10}) of the forest floor community vary amongst the sites, since the respiration activity of soil microbial communities (Briones and others 2014) and plants (Tjoelker and others 2008) can acclimate under different conditions. For instance, FET (215 years since fire) consistently experienced higher average annual temperatures than other sites (data not shown) and had the lowest ER and CH_4 consumption in July 2014 (Figure 2), which was much warmer and drier than the other sampling periods. It is possible that the microbial community at FET is less sensitive to warmer temperatures than those at other sites and therefore had a smaller response to higher temperatures. In relation to this, sampling period was highly significant in ER, NEE, and CH_4 fluxes, highlighting the importance of overall climatic conditions at the time of sampling. Again, evidence of this was seen in July 2014, which had higher ER and NEE fluxes as well as higher CH_4 consumption corresponding to warm, dry conditions (Figure 2). Notably, compared to other sites, the youngest site (NJA, 47 years since fire) had exceptionally low (i.e. highly negative) NEE linked to high photosynthetic activity during this period. This is likely the result of higher grass biomass (data not shown), which is much faster-growing than the feathermoss or shrub species.

Ecosystem respiration showed a strong positive response to soil moisture, which is known to be important for microbial activity and plant productivity in boreal systems (Williams and Flanagan 1996; DeLuca and Boisvenue 2012; Van Cleve and Sprague 2015). Although soil moisture, a driver of methane oxidation in boreal soils (McNamara and others 2015), did not appear to influence our CH_4 fluxes, increases in leaf moisture were associated with greater CH_4 influx. Leaf and soil moisture were both significantly linked to N_2O fluxes; however, this model had a very low R^2 value, resulting in low confidence in its use as a predictor of N_2O fluxes and highlighting the complexity of the N cycle in this system.

Neither total aboveground biomass nor percent cover of *P. schreberi* had any significant effect on greenhouse gas fluxes in our models. We expected that N_2O emissions would increase as feathermoss abundance (and associated N_2-fixation) has been shown to increase with TSF in these stands (Zackrisson and others 2004) and because feathermosses such as *H. splendens* have been shown to release N_2O (Lenhart and others 2015). It is possible that a decrease in nitrification and ammonification in the soil (DeLuca and others 2002a) counteracted this somewhat, but also the *P. schreberi* cover in our plots only ranged from 70-100%, which may not have been enough variation to see an effect. Future work might include measurements of these processes along with N_2O emissions to explore this further.

In this heterogeneous, high latitude landscape, micro-topography can greatly influence site conditions and microclimate; for example, the low solar angle means that slope and aspect influence how much solar radiation a stand can receive (Bonan and Shugart 1989). Similarly, Zackrisson (1977) noted that stands on south-facing slopes in the Swedish boreal region experience more frequent fires than those facing north. Several other factors contributing to soil and plant community compositions following wildfire are important considerations. The intensity and severity of the burn greatly impact secondary succession by influencing forest structure and the remaining nutrient pool (Flannigan and others 2005; Lecomte and others 2006). For example, we know NJA (47 years since fire) experienced a high severity, stand-replacing fire and now has much higher grass cover (data not shown) and fewer trees (personal observation) than JAR, which burned only six years earlier. Moreover, stand structure prior to burning partially dictates how severe the next fire might be (i.e. recently burned stands with less organic material accumulated will likely experience a less severe burn than an old site with abundant fuel). As well, the amount of charcoal remaining is important for enhancing soil fertility and adsorption of allelopathic polyphenols following fire (Zackrisson and others 1996; DeLuca and others 2002a). Future work on *in situ* boreal forest floor GHG fluxes would benefit from measures of these factors.

Conclusion

We predicted that there would be trends in soil properties, *P. schreberi* cover, and microbial communities with increasing time since last wildfire disturbance and that these properties would influence GHG emissions along our chronosequence. Our results show that boreal forest floor GHG emissions are both site- and climate-driven, where site encompasses combinations of measured and unmeasured factors (such as the intensity and severity of the last burn, the structure of the forest prior to burning and adjacent to burn sites, and the amount of charcoal remaining). Climate, as indicated by sampling period, was a strong driver of GHG fluxes but some soil properties (C:N, depth, and moisture) were influential. Many studies show trends in ecosystem properties along boreal forest wildfire chronosequences, but our study suggests that local heterogeneity in the landscape is a powerful regulator of later successional forest floor GHG emissions and needs to be considered when predicting the effects of more frequent, severe and extensive wildfires.

Acknowledgements

Funding for this research was provided by the Natural Environment Research Council, UK. We would like to thank T. N. Walker, P. A. Henrys, and S. G. Jarvis for their guidance in statistical analyses and use of R software, and Matt Clifford for his assistance in the laboratory analyses. Special thanks to the kind staff at the Silvermuseet in Arjeplog for letting us share their space.

References:

Allison SD, Czimczik CI, Treseder KK. 2008. Microbial activity and soil respiration under nitrogen addition in Alaskan boreal forest. Global Change Biology 14:1156–68.

Bartoń K. 2016. MuMIn: Multi-Model Interface. R package version 1.15.6.

Bligh EG, Dyer WJ. 1959. A rapid method of total lipid extraction and purification. Canadian Journal of Biochemistry and Physiology 37:911–7.

Bonan GB, Shugart HH. 1989. Environmental Factors and Ecological Processes in Boreal Forests. Annual Review of Ecology and Systematics 20:1–28.

Brais S, Camiré C, Bergeron Y, Paré D. 1995. Changes in nutrient availability and forest floor characteristics in relation to stand age and forest composition in the southern part of the boreal forest of northwestern Quebec. Forest Ecology and Management 76:181–9.

Briones MJI, McNamara NP, Poskitt J, Crow SE, Ostle NJ. 2014. Interactive biotic and abiotic regulators of soil carbon cycling: Evidence from controlled climate experiments on peatland and boreal soils. Global Change Biology 20:2971–82.

Carcaillet C, Bergman I, Delorme S, Hornberg G, Zackrisson O. 2007. Long-term fire frequency not linked to prehistoric occupation in northern Swedish boreal forest. Ecology 88:465–77.

Chapin FS III, Matson PA, Mooney HA. 2002. Princples of Terrestrial Ecosystem Ecology. New York: Springer. 436 p.

Clemmensen KE, Bahr A, Ovaskainen O, Dahlberg A, Ekblad A, Wallander H, Stenlid J, Finlay RD, Wardle DA, Lindahl BD. 2013. Roots and Associated Fungi Drive Long-Term Carbon Sequestration in Boreal Forest. Science 339:1615–8.

Clemmensen KE, Finlay RD, Dahlberg A, Stenlid J, Wardle DA, Lindahl BD. 2015. Carbon sequestration is related to mycorrhizal fungal community shifts during long-term succession in boreal forests. New Phytologist 205:1525–36.

Crossman ZM, Abraham F, Evershed RP. 2004. Stable Isotope Pulse-Chasing and Compound Specific Stable Carbon Isotope Analysis of Phospholipid Fatty Acids to Assess Methane Oxidizing Bacterial Populations in Landfill Cover Soils. Environmental Science and Technology 38:1359–67.

de Groot WJ, Flannigan MD, Cantin AS. 2013. Climate change impacts on future boreal fire regimes. Forest Ecology and Management 294:35–44.

de Vries FT, Manning P, Tallowin JRB, Mortimer SR, Pilgrim ES, Harrison KA, Hobbs PJ, Quirk H, Shipley B, Cornelissen JHC, Kattge J, Bardgett RD. 2012. Abiotic drivers and plant traits explain landscape-scale patterns in soil microbial communities. Ecology Letters 15:1230–9.

DeLuca TH, Nilsson M-C, Zackrisson O. 2002a. Nitrogen mineralization and phenol accumulation along a fire chronosequence in northern Sweden. Oecologia 133:206–14.

DeLuca TH, Zackrisson O, Nilsson M-C, Sellstedt A. 2002b. Quantifying nitrogen-fixation in feather moss carpets of boreal forests. Letters to Nature 419:917–20.

DeLuca TH, Sala A. 2006. Frequent Fire Alters Nitrogen Transformations in Ponderosa Pine Stands of the Inland Northwest. Ecology 87:2511–22.

DeLuca TH, Zackrisson O, Gundale MJ, Nilsson M-C. 2008. Ecosystem feedbacks and nitrogen fixation in boreal forests. Science 320:1181.

DeLuca TH, Boisvenue C. 2012. Boreal forest soil carbon: Distribution, function and modelling. Forestry 85:161–84.

Engelmark O. 1999. Boreal forest disturbance. In: R. L. Walker, editor. Ecosystems of disturbed ground. Volume 16 of Ecosystems of the World. Elsevier, Burlington, USA. p161–186.

Flannigan MD, Amiro BD, Logan KA, Stocks BJ, Wotton BM. 2005. Forest Fires and Climate Change in the 21ST Century. Mitigation and Adaptation Strategies for Global Change 11:847–59.

Flannigan M, Cantin AS, De Groot WJ, Wotton M, Newbery A, Gowman LM. 2013. Global wildland fire season severity in the 21st century. Forest Ecology and Management 294:54–61.

Girardin MP, Ali A, Carcaillet C, Mudelsee M, Drobyshev I, Hély C, Bergeron Y. 2009. Heterogeneous response of circumboreal wildfire risk to climate change since the early 1900s. Global Change Biology 15:2751–69.

Harden JW, Mack M, Veldhuis H, Gower ST. 2002. Fire dynamics and implications for nitrogen cycling in boreal forests. Journal of Geophysical Research 108:8223.

Hobbie SE, Nadelhoffer KJ, Högberg P. 2002. A synthesis: The role of nutrients as constraints on carbon balances in boreal and arctic regions. Plant and Soil 242:163–70.

Holden SR, Gutierrez A, Treseder KK. 2013. Changes in Soil Fungal Communities, Extracellular Enzyme Activities, and Litter Decomposition Across a Fire Chronosequence in Alaskan Boreal Forests. Ecosystems 16:34–46.

Jonasson S, Michelsen A, Schmidt IK, Nielsen EV. 1999. Responses in microbes and plants to changed temperature, nutrient, and light regimes in the arctic. Ecology 80:1828–43.

Kovats, RS, Valentini R, Bouwer LM, Georgopoulou E, Jacob D, Martin E, Rounsevell M, Soussana J-F. 2014. Europe. In: Barros VR, Field CB, Dokken DJ, Mastrandrea MD, Mach KJ, Bilir TE, Chatterjee M, Ebi KL, Estrada YO, Genova RC, Girma B, Kissel ES, Levy AN, MacCracken S, Mastrandrea PR, White LL, editors. Climate Change 2014: Impacts, Adaptation, and Vulnerability. Part B: Regional Aspects. Contribution of Working Group II to the Fifth Assessment Report of the Intergovernmental Panel on Climate Change. Cambridge, UK and New York, USA: Cambridge University Press. p1267–1326.

Lagerström A, Esberg C, Wardle DA, Giesler R. 2009. Soil phosphorus and microbial response to a long-term wildfire chronosequence in northern Sweden. Biogeochemistry 95:199–213.

Lecomte N, Simard M, Fenton N, Bergeron Y. 2006. Fire Severity and Long-term Ecosystem Biomass Dynamics in Coniferous Boreal Forests of Eastern Canada. Ecosystems 9:1215–30.

Lenhart K, Weber B, Elbert W, Steinkamp J, Clough T, Crutzen P, Pöschl U, Keppler F. 2015. Nitrous oxide and methane emissions from cryptogamic covers. Global Change Biology 21: 3889–3900.

McNamara NP, Gregg R, Oakley S, Stott A, Rahman MT, Murrell JC, Wardle DA, Bardgett RD, Ostle NJ. 2015. Soil Methane Sink Capacity Response to a Long-Term Wildfire Chronosequence in Northern Sweden. PLoS ONE 10:e0129892.

Niklasson M, Granstrom A. 2013. Numbers and Sizes of Fires : Long-Term Spatially Explicit Fire History in a Swedish Boreal Landscape. Ecology 81:1484–99.

Oechel WC, Van Cleve K. 1986. The Role of Bryophytes in Nutrient Cycling in the Taiga. In: Van Cleve K, Chapin FS, Flanagan PW, Viereck LA, Dyrness CT, editors. Forest Ecosystems in the Alaskan Taiga: A Synthesis of Structure and Function. New York: Springer-Verlag New York. p121–37.

O'Neill KP, Kasischke ES, Richter DD. 2003. Seasonal and decadal patterns of soil carbon uptake and emission along an age sequence of burned black spruce stands in interior Alaska. Journal of Geophysical Research 108:8155.

Pan Y, Birdsey RA, Fang J, Houghton R, Kauppi PE, Kurz WA, Phillips OL, Shvidenko A, Lewis SL, Canadell JG, Ciais P, Jackson RB, Pacala SW, McGuire AD, Piao S, Rautiainen A, Sitch S, Hayes D. 2011. A large and persistent carbon sink in the world's forests. Science 333:988–93.

Paré D, Bergeron Y, Camiré C. 1993. Changes in the Forest Floor of Canadian Southern Boreal Forest after Disturbance. Journal of Vegetation Science 4:811–8.

Pinheiro J, Bates D, DebRoy S, Sarkar D, R Core Team. 2015. nlme: Linear and Nonlinear Mixed Effects Models. R package version 3.1-122.

Prescott CE, Maynard DG, Laiho R. 2000. Humus in northern forests: Friend or foe? Forest Ecology and Management 133:23–36.

R Development Core Team. 2014. R: A language and environment for statistical computing. R Foundation for Statistical Computing, Vienna, Austria. (Available at: http://www.R-project.org/).

Street LE, Subke J-A, Sommerkorn M, Sloan V, Ducrotoy H, Phoenix GK, Williams M. 2013. The role of mosses in carbon uptake and partitioning in arctic vegetation. New Phytologist 199:163–75.

Tjoelker MG, Oleksyn J, Reich PB, Żytkowiak R. 2008. Coupling of respiration, nitrogen, and sugars underlies convergent temperature acclimation in Pinus banksiana across wide-ranging sites and populations. Global Change Biology 14:782–97.

Van Cleve K, Sprague D. 2015. Respiration rates in the forest floor of birch and aspen stands in interior Alaska. Journal of Canadian Forest Research 3:17–26.

Ward C, Pothier D, Paré D. 2014. Do boreal forests need fire disturbance to maintain productivity? Ecosystems 17:1053–1067.

Ward SE, Ostle NJ, Oakley S, Quirk H, Henrys PA, Bardgett RD. 2013. Warming effects on greenhouse gas fluxes in peatlands are modulated by vegetation composition. Ecology Letters 16:1285–93.

Wardle DA. 1997. The Influence of Island Area on Ecosystem Properties. Science 277:1296–9.

Wardle DA, Hörnberg G, Zackrisson O, Kalela-Brundin M, Coomes DA. 2003. Long-term effects of wildfire on ecosystem properties across an island area gradient. Science 300:972–5.

Wardle DA, Zackrisson O. 2005. Effects of species and functional group loss on island ecosystem properties. Nature 435:806–10.

Wardle DA, Jonsson M, Bansal S, Bardgett RD, Gundale MJ, Metcalfe DB. 2012a. Linking vegetation change, carbon sequestration and biodiversity: Insights from island ecosystems in a long-term natural experiment. Journal of Ecology 100:16–30.

Wardle DA, Jonsson M, Kalela-Brundin M, Lagerström A, Bardgett RD, Yeates GW, Nilsson MC. 2012b. Drivers of inter-year variability of plant production and decomposers across contrasting island ecosystems. Ecology 93:521–31.

Whitaker J, Ostle N, Nottingham AT, Ccahuana A, Salinas N, Bardgett RD, Meir P, McNamara NP. 2014. Microbial community composition explains soil respiration responses to changing carbon inputs along an Andes-to-Amazon elevation gradient. Journal of Ecology 102:1058–71.

Williams TG, Flanagan LB. 1996. Effect of changes in water content on photosynthesis, transpiration and discrimination against $^{13}CO_2$ and $C^{18}O^{16}O$ in Pleurozium and Sphagnum. Oecologia 2:38–46.

Zackrisson O. 1977. Influence of forest fires on the North Swedish boreal forest. Oikos 29:22–32.

Zackrisson O. 1980. Forest fire history: ecological significance and dating problems in the north Swedish boreal forests. - In: Dietrich, JH, Stokes, M, editors. Proceedings of the fire history workshop, University of Arizona. USDA, Rocky Mountain Forest and Experiment Station. General Technical Report RM81, p120–125.

Zackrisson O, Nilsson M, Wardle DA. 1996. Ecological Function of Charcoal from Wildfire in the Boreal Forest. Oikos 77:10–9.

Zackrisson O, DeLuca TH, Nilsson MC, Sellstedt A, Berglund LM. 2004. Nitrogen fixation increases with successional age in boreal forests. Ecology 85:3327–34.

Zackrisson O, DeLuca TH, Gentili F, Sellstedt A, Jäderlund A. 2009. Nitrogen fixation in mixed Hylocomium splendens moss communities. Oecologia 160:309–19.

Zuur AE, Ieno EN, Walker NJ, Saveliev AA, Smith GM. 2009. Mixed Effects Models and Extensions in Ecology with R. New York: Springer. 574p.

Figure Captions

Figure 1. Significant (linear regression with time since fire) soil properties of the organic horizon sampled within the gas chamber rings (blue circles) and along a separate transect (black dots) at selected sites; dw = dry weight.

Figure 2. Mean greenhouse gas fluxes (± standard error) in each sampling campaign.

Figure S1. Non-significant (linear regression with time since fire) soil properties of the organic horizon samples within the gas chamber rings (blue circles) and along a separate transect (black dots) at selected sites; dw = dry weight, SOM = soil organic matter, PLFA = phospholipid fatty acid.

Figure S2. Linear regression results of final plant aboveground biomass and percent cover of *Pleurozium schreberi* in the field plots at selected sites.

Table 1. Summary information for sampling locations. Site ages are the time since fire as of 2014.

Site name	Site code	Location	Time since fire (years)
Njållatjivelg	NJA	65° 48′ 54″ N 19° 02′ 07″ E	47
Jarvliden	JAR	65° 34′ 09″ N 18° 24′ 01″ E	53
Laddok	LAD	65° 56′ 43″ N 18° 22′ 37″ E	136
Guorbåive	GUO	65° 48′ 57″ N 19° 02′ 54″ E	183
Fettjärn	FET	65° 55′ 28″ N 18° 29′ 58″ E	232
Reivo	REV	65° 46′ 28″ N 19° 06′ 19″ E	367

Table 2. Summary of fixed factors initially included for LME model selection.

Factors Included in Model Selection	Mean	Standard Error	Range
Site (or Time Since Fire)* Soil Temperature (5 cm depth)	-	-	-
Site (or Time Since Fire)	169.67 years	23.18 years	47 – 367 years
Soil Temperature (5 cm depth)	9.26°C	0.60°C	5.26 – 15.78°C
Sampling Period	-	-	-
Photosynthetically Active Radiation (PAR)	79.41 µmol m^{-2} s^{-1}	38.47 µmol m^{-2} s^{-1}	2 – 1130 µmol m^{-2} s^{-1}
Soil Moisture	24%	1%	4 – 33%
Leaf Moisture	514.81 raw counts	25.27 raw counts	437 – 909.83 raw counts
$Depth_{OH}$	5.82 cm	0.57 cm	1.5 – 10.5 cm
$C:N_{OH}$	34.90	0.90	19.99 – 48.14
Total N_{OH}	7.15 mg g^{-1} soil	0.40 mg g^{-1} soil	2.74 – 12.54 mg g^{-1} soil
Final Aboveground Biomass	149.69 g	5.71 g	84.1 – 208.40 g
% Cover - *Pleurozium schreberi*	95.5%	1.39%	70 – 100%

After removal of collinear terms, these factors were included in the initial linear mixed effects models and subject to removal using a step-wise process. OH = Soil organic horizon.

Table 3. Likelihood ratio deletion test results for selected models of greenhouse gas fluxes

		Ecosystem Respiration	**Net Ecosystem Exchange**	**CH_4 Flux**	**N_2O Flux**
		$R^2_{marginal} = 0.642$ $R^2_{conditional} = 0.679$ RMSE = 1.338	$R^2_{marginal} = 0.397$ $R^2_{conditional} = 0.489$ RMSE = 24.589	$R^2_{marginal} = 0.299$ $R^2_{conditional} = 0.608$ RMSE = 0.022	$R^2_{marginal} = 0.040$ $R^2_{conditional} = 0.040$ RMSE = 0.005
Factor	Site*Soil Temperature$_{5cm}$	-	17.86, *df* = 15,20, $p < 0.0013$	-	-
	Site	21.24, *df* = 11,17, $p < 0.0003$	18.95, *df* = 10,16, $p < 0.0008$	12.38, *df* = 9,15, $p < 0.0148$	10.06, *df* = 6,13, $p < 0.0394$
	Soil Temperature$_{5cm}$	-	5.13, *df* = 10,16, $p = 0.0236$	-	-
	Sampling Period	81.87, *df* = 11,17, $p < 0.0001$	32.08, *df* = 15,20, $p < 0.0001$	43.54, *df* = 9,15, $p < 0.0001$	-
	PAR	-	-	-	-
	Soil Moisture	22.78, *df* = 11,17, $p < 0.0001$	-	-	6.02, *df* = 6,13, $p < 0.0141$
	Leaf Moisture	24.80, *df* = 11,17, $p < 0.0001$	-	7.07, *df* = 9,15, $p < 0.0078$	8.19, *df* = 6,13, $p < 0.0042$
	Depth$_{OH}$	-	8.55, *df* = 15,20, $p < 0.0035$	-	-
	C:N$_{OH}$	4.72, *df* = 11,17, $p < 0.0299$	-	-	-
	Total N$_{OH}$	-	-	-	-
	Final Plant Biomass	-	-	-	-
	% Cover – *P. schreberi*	-	-	-	-

*Likelihood ratio deletion test results (LR, degrees of freedom (*df*), *p*-value) and model fit (marginal and conditional R^2, root mean square error (RMSE)) of linear mixed effects models of greenhouse gas (GHG) fluxes. The final model for each GHG was selected based on a step-wise routine using single term deletions combined with likelihood ratio testing. The LR and p-values for each variable are the results of likelihood ratio tests between the maximum likelihood estimations of the final model and the same final model with that variable removed. R^2 values and RMSE are from final models with restricted maximum likelihood estimations. PAR = photosynthetically active radiation, OH = soil organic horizon.*

Table 4. Parameter estimates for selected LME models of greenhouse gas fluxes

		Ecosystem Respiration		**Net Ecosystem Exchange**		**CH_4 Flux**		**N_2O Flux**	
		Parameter estimate (± SE)	*p*-value	Parameter estimate (± SE)	*p*-value	Parameter estimate (± SE)	*p*-value	Parameter estimate (± SE)	*p*-value
Factor	Intercept	3. 924 ± 2.067	0.0606	27.686 ± 28.821	0.3389	-0.010 ± 0.013	0.4331	0.00264 (± 0.00281)	0.3497
	Site*Soil Temperature$_{5cm}$	-	-			-	-	-	-
	JAR*Soil Temperature$_{5cm}$	-	-	7.425 ± 2.119	0.0007	-	-	-	-
	LAD*Soil Temperature$_{5cm}$	-	-	15.938 ± 4.911	0.0016	-	-	-	-
	FET*SoilTemperature$_{5cm}$	-	-	3.592 ± 2.317	0.1240	-	-	-	-
	REV*SoilTemperature$_{5cm}$	-	-	5.567 ± 2.281	0.0163	-	-	-	-
	Site								
	JAR	-0.917 ± 0.552	0.1133	-27.353 ± 21.266	0.2138	0.006 ± 0.013	0.6619	-0.00060 (± 0.00165)	0.7206
	LAD	0.752 ± 0.627	0.2455	-111.812 ± 39.599	0.0109	0.007 ± 0.013	0.5946	-0.00226 (± 0.00170)	0.1999
	FET	3.228 ± 0.955	0.0032	19.294 ± 24.358	0.4381	0.040 ± 0.012	0.0043	-0.00577 (± 0.00198)	0.0087
	REV	-0.286 ± 0.490	0.5666	-26.392 ± 23.237	0.2702	0.018 ± 0.012	0.1532	-0.00146 (± 0.00158)	0.3648
	Soil Temperature$_{5cm}$	-	-	-0.658 ± 3.140	0.8344	-	-	-	-
	Sampling Period							-	-
	Sept 2012	-1.752 ± 0.419	0.0001	-12.619 ± 8.270	0.1300	-0.016 ± 0.005	0.0012	-	-
	June 2013	0.059 ± 0.457	0.8975	-47.146 ± 7.752	<0.0001	-0.010 ± 0.006	0.0656	-	-
	July 2014	3.813 ± 0.544	<0.0001	-32.776 ± 14.908	0.0301	-0.036 ± 0.005	<0.0001	-	-
	PAR	-	-	-	-	-	-	-	-
	Soil Moisture	28.662 ± 5.698	<0.0001	-	-	-	-	-0.02417 ± 0.00994	0.0166
	Leaf Moisture	-0.006 ± 0.001	<0.0001	-	-	$-4.0 \times 10^{-5} \pm 1.5 \times 10^{-5}$	0.0072	$9.91 \times 10^{-5} \pm 3.38 \times 10^{-6}$	0.0041
	Depth$_{OH}$	-	-	-5.213 ± 1.847	0.0109	-	-	-	-
	C:N$_{OH}$	-0.067 ± 0.032	0.0545	-	-	-	-	-	-
	Total N$_{OH}$	-	-	-	-	-	-	-	-
	Final Plant Biomass	-	-	-	-	-	-	-	-
	% Cover – *P. schreberi*	-	-	-	-	-	-	-	-

Parameter estimates and p-values (restricted maximum likelihood estimated models) are based on comparisons to the intercept, which includes site NJA and sampling period June 2012. PAR= photosynthetically active radiation, OH = soil organic horizon.

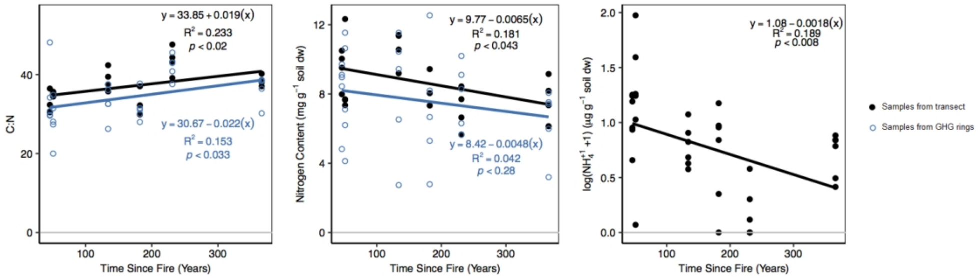

Figure 1. Significant (linear regression with time since fire) soil properties of the organic horizon sampled within the gas chamber rings (blue circles) and along a separate transect (black dots) at selected sites; dw = dry weight.

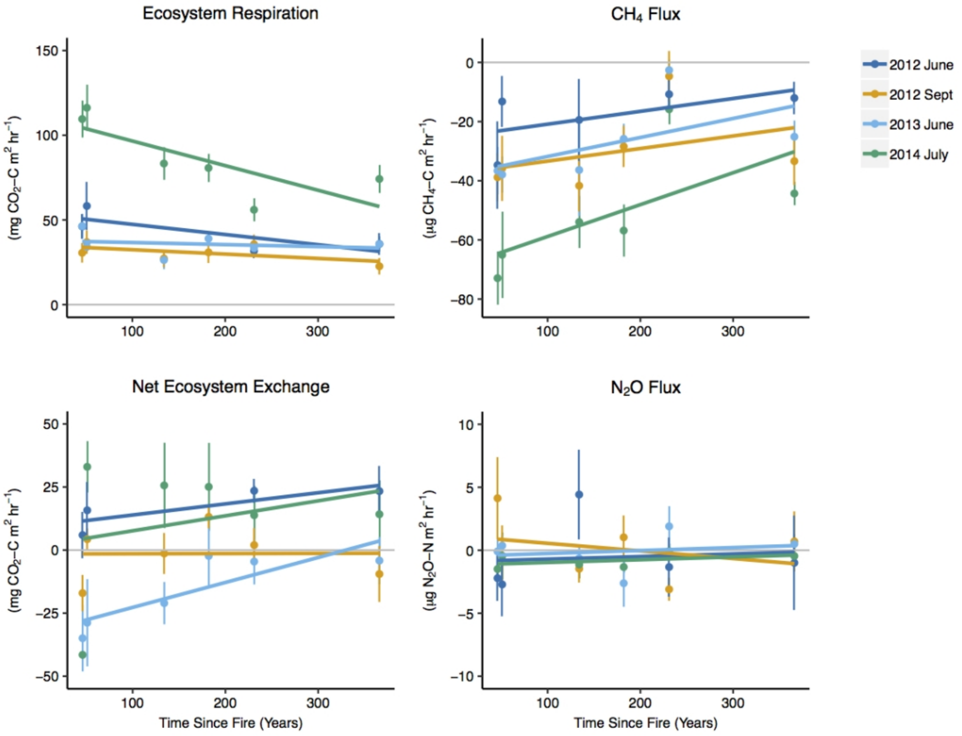

Figure 2. Mean greenhouse gas fluxes (± standard error) in each sampling campaign.

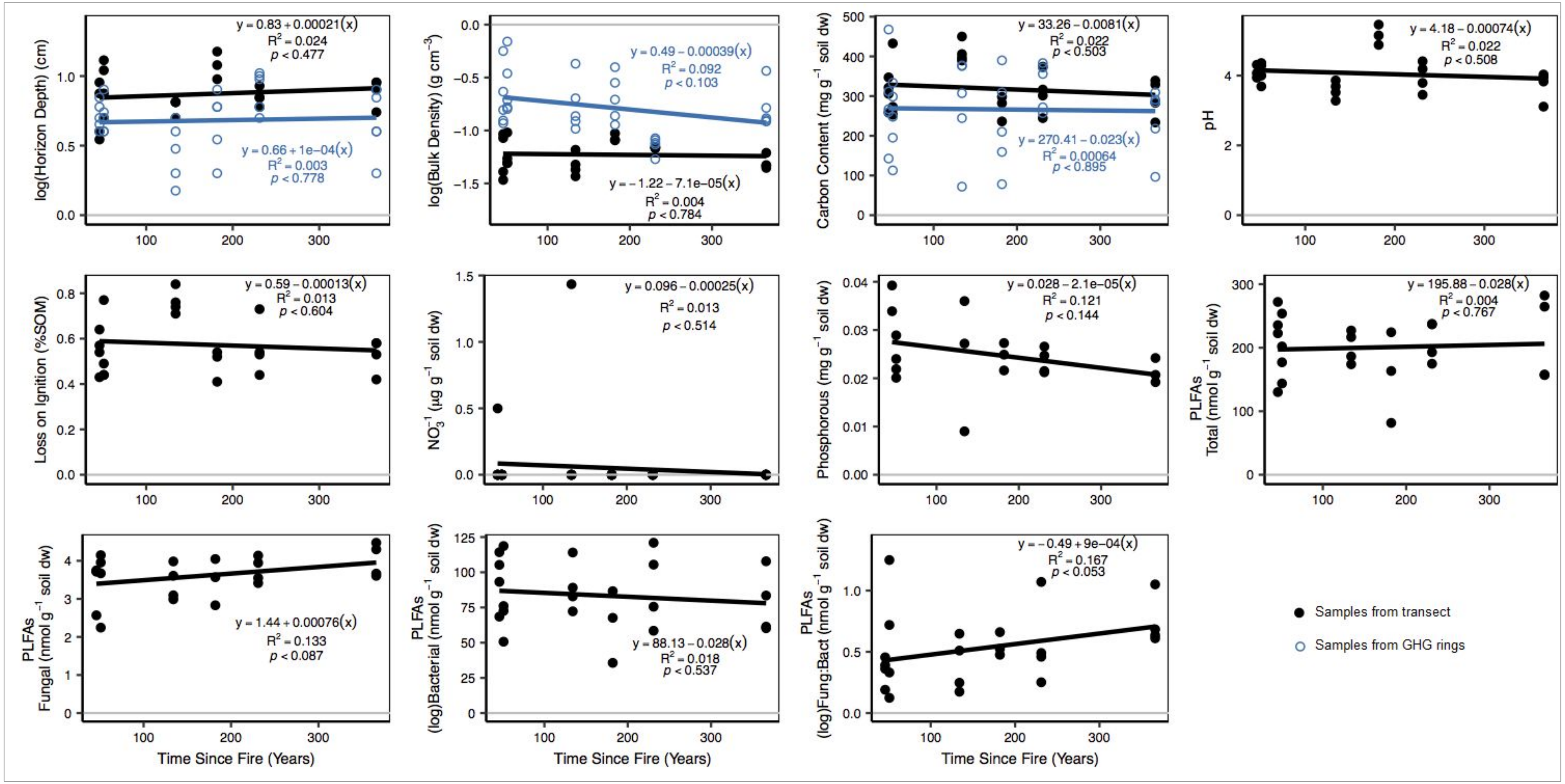

Figure S1. Non-significant (linear regression with time since fire) soil properties of the organic horizon samples within the gas chamber rings (blue circles) and along a separate transect (black dots) at selected sites; dw = dry weight, SOM = soil organic matter, PLFA = phospholipid fatty acid.

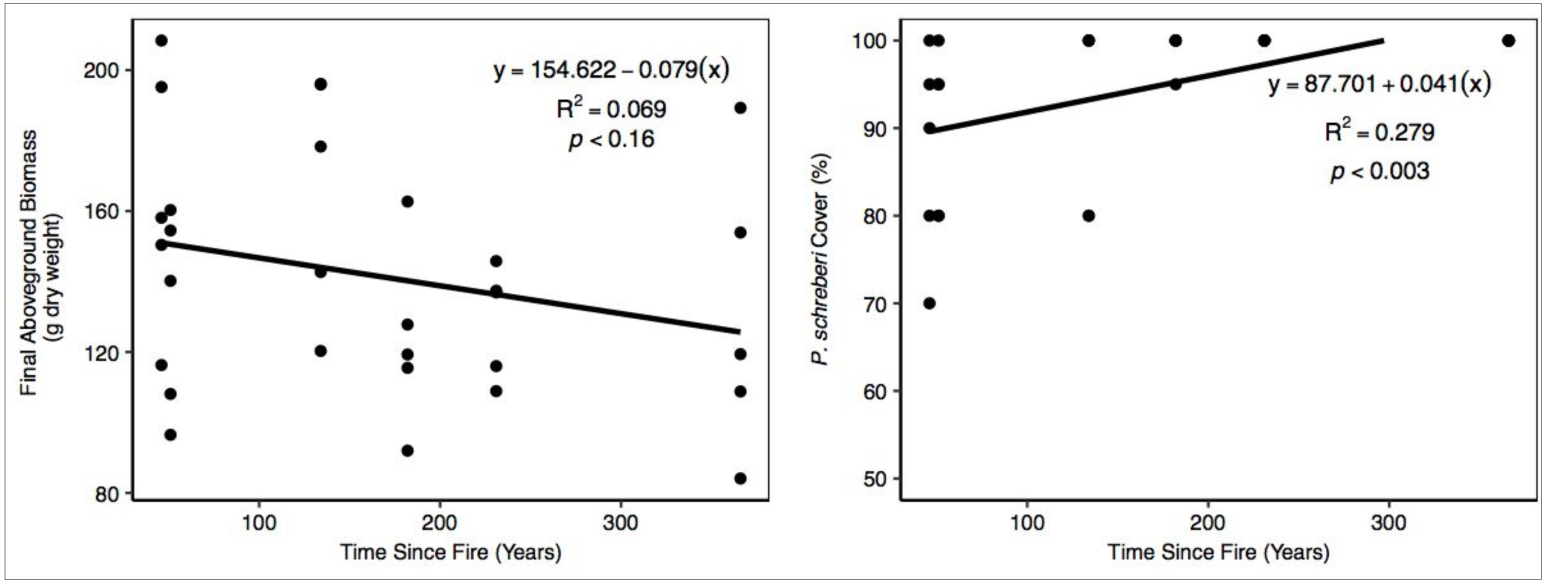

Figure S2. Linear regression results of final plant aboveground biomass and percent cover of *Pleurozium schreberi* in the field plots at selected sites.

Table S1. Likelihood ratio deletion test results for selected models of greenhouse gas fluxes (using time since fire in fixed effects selection)

		Ecosystem Respiration	**Net Ecosystem Exchange**	**CH_4 Flux**	**N_2O Flux**
		$R^2_{marginal}$ = 0.593 $R^2_{conditional}$ = 0.666 RMSE = 1.434	$R^2_{marginal}$ = 0.136 $R^2_{conditional}$ = 0.335 RMSE = 28.654	$R^2_{marginal}$ = 0.307 $R^2_{conditional}$ = 0.601 RMSE = 0.022	No significant model
Factor	Time Since Fire*Soil $Temperature_{5cm}$	-	-	-	-
	Time Since Fire	-	-	-	-
	Soil $Temperature_{5cm}$	-	7.55, *df* = 4,11, *p* = 0.0060	-	-
	Sampling Period	92.72, *df* = 5,12, *p* < 0.0001	26.49, *df* = 4,11, *p* < 0.0001	42.85, *df* = 9,16, *p* < 0.0001	-
	PAR	-	-	-	-
	Soil Moisture	93.08, *df* = 5,12, *p* < 0.0001	-	-	-
	Leaf Moisture	105.68, *df* = 5,12, *p* < 0.0001	-	7.26, *df* = 9,16, *p* = 0.0007	-
	$Depth_{OH}$	-	-	-	-
	$C:N_{OH}$	-	-	7.90, *df* = 9,16, *p* = 0.0049	-
	Total N_{OH}	-	-	4.87, *df* = 9,16, *p* = 0.0273	-
	Final Plant Biomass	-	-	-	-
	% Cover – *P. schreberi*	-	-	-	-

*Likelihood ratio deletion test results (LR, degrees of freedom (*df*), p-value) and model fit (marginal and conditional R^2, root mean square error (RMSE)) of linear mixed effects models of greenhouse gas (GHG) fluxes where time since fire was included in fixed effects selection. The final model for each GHG was selected based on a step-wise routine using single term deletions combined with likelihood ratio testing. The LR and p-values for each variable are the results of likelihood ratio tests between the maximum likelihood estimations of the final model and the same final model with that variable removed. R^2 values and RMSE are from final models with restricted maximum likelihood estimations. PAR = photosynthetically active radiation, OH = soil organic horizon.*

Table S2. Parameter estimates for selected LME models of greenhouse gas fluxes (using time since fire in fixed effects selection)

		Ecosystem Respiration – Log$_{10}$		**Net Ecosystem Exchange**		**CH$_4$ Flux**		**N$_2$O Flux**	
		Parameter estimate (± SE)	*p*-value	Parameter estimate (± SE)	*p*-value	Parameter estimate (± SE)	*p*-value	Parameter estimate (± SE)	*p*-value
Factor	Intercept	5.649 ± 1.024	<0.0001	-40.583 ± 20.503	0.0602	-0.046 ± 0.023	0.0539	-	-
	Time Since Fire*Soil Temperature$_{5cm}$	-	-	-	-	-	-	-	-
	Time Since Fire	-	-	-	-	-	-	-	-
	Soil Temperature$_{5cm}$	-	-	6.658 ± 2.266	0.0040	-	-	-	-
	Sampling Period							-	-
	Sept 2012	-1.577 ± 0.419	0.0003	-6.555 ± 8.525	0.4436	-0.015 ± 0.005	0.0013	-	-
	June 2013	-0.391 ± 0.449	0.3852	-39.028 ± 7.722	<0.0001	-0.010 ± 0.006	0.0688	-	-
	July 2014	2.924 ± 0.486	<0.0001	-42.874 ± 14.422	0.0036	-0.036 ± 0.005	<0.0001	-	-
	PAR	-	-	-	-	-	-	-	-
	Soil Moisture	13.270 ± 2.862	<0.0001	-	-	-	-	-	-
	Leaf Moisture	-0.005 ± 0.001	<0.0001	-	-	$-4.08 \times 10^{-5} \pm 1.47 \times 10^{-5}$	0.0066	-	-
	Depth$_{OH}$	-	-			-	-	-	-
	C:N$_{OH}$	-		-	-	0.0017 ± 0.0006	0.0086	-	-
	Total N$_{OH}$	-	-	-	-	-0.0008 ± 0.0004	0.0405	-	-
	Final Plant Biomass	-	-	-	-	-	-	-	-
	% Cover – *P. schreberi*	-	-	-	-	-	-	-	-

Parameter estimates and p-values (restricted maximum likelihood estimated models) are based on comparisons to the intercept, which includes sampling period June 2012. PAR= photosynthetically active radiation, OH = soil organic horizon.